Interaction of jack bean (*Canavalia ensiformis*) urease and a derived peptide with lipid vesicles

Yasmine Miguel Serafini Micheletto [a,1], Carlo Frederico Moro [b,1],
Fernanda Cortez Lopes [d,e], Rodrigo Ligabue-Braun [b], Anne Helene Souza Martinelli [e],
Carlos Manuel Marques [c], André Pierre Schroder [c], Célia Regina Carlini [b,d,e,*],
Nádya Pesce da Silveira [a,**]

[a] Graduate Program in Chemistry, Institute of Chemistry, Universidade Federal do Rio Grande do Sul, Porto Alegre, RS, Brazil
[b] Graduate Program in Cellular and Molecular Biology, Center of Biotechnology, Universidade Federal do Rio Grande do Sul, Porto Alegre, RS, Brazil
[c] Institut Charles Sadron, Université de Strasbourg, UPR22-CNRS, Strasbourg, France
[d] Instituto do Cérebro, Pontífica Universidade Católicado Rio Grande do Sul, Porto Alegre, RS, Brazil
[e] Department of Biophysics, Universidade Federal do Rio Grande do Sul, Porto Alegre, RS, Brazil

ARTICLE INFO

ABSTRACT

Ureases are metalloenzymes that catalyze the hydrolysis of urea to ammonia and carbon dioxide. Jack bean (*Canavalia ensiformis*) produces three isoforms of urease (Canatoxin, JBU and JBURE-II). Canatoxin and JBU display several biological properties independent of their ureolytic activity, such as neurotoxicity, exocytosis-inducing and pro-inflammatory effects, blood platelets activation, insecticidal and antifungal activities. The Canatoxin entomotoxic activity is mostly due to an internal peptide, named pepcanatox, released upon the hydrolysis of the protein by insect cathepsin-like digestive enzymes. Based on pepcanatox sequence, Jaburetox-2Ec was produced in *Escherichia coli*. JBU and its peptides were shown to permeabilize membranes through an ion channel-based mechanism. Here we studied the JBU and Jaburetox-2Ec interaction with platelet-like multilamellar liposomes (PML) using Dynamic Light Scattering and Small Angle X-ray Scattering techniques. We also analyzed the interaction of JBU with giant unilamellar vesicles (GUVs) using Fluorescence Microscopy. The interaction of vesicles with JBU led to a slight reduction of hydrodynamic radius, and caused an increase in the lamellar repeat distance of PML, suggesting a membrane disordering effect. In contrast, Jaburetox-2Ec decreased the lamellar repeat distance of PML membranes, while also diminishing their hydrodynamic radius. Fluorescence microscopy showed that the interaction of GUVs with JBU caused membrane perturbation with formation of tethers. In conclusion, JBU can interact with PML, probably by inserting its Jaburetox "domain" into the PML external membrane. Additionally, the interaction of Jaburetox-2Ec affects the vesicle's internal bilayers and hence causes more drastic changes in the PML membrane organization in comparison with JBU.

© 2016 Elsevier B.V. All rights reserved.

1. Introduction

Ureases are nickel-dependent metalloenzymes that catalyze the hydrolysis of urea to form ammonia and carbon dioxide [1]. Jack bean urease (JBU) isolated from *Canavalia ensiformis* seeds was the first enzyme to be crystallized in 1926 by Sumner [2] and its crystallographic structure was elucidated only 83 years later by Balasubramanian et al., 2010 [3]. JBU consists of identical ~90 kDa subunits, containing two nickel ions each, which in the native enzyme associate into trimers or hexamers [4]. *C. ensiformis* has three isoforms of urease: JBU, Jack bean urease II (JBURE-II) and Canatoxin [5,6]. Previous studies have shown that Canatoxin and JBU, besides their ureolytic activity, also display other biological properties, such as neurotoxicity, exocytosis-inducing and pro-inflammatory effects, activation of blood platelets, and insecticidal and antifungal activities [5,7–11].

The Canatoxin entomotoxic activity is mostly due to an internal peptide, named pepcanatox, released upon the protein hydrolysis by insect cathepsin-like digestive enzymes [12–14]. Based on the N-terminal sequence of pepcanatox, an analogous peptide was cloned based on the JBURE-II sequence and expressed in *Escherichia coli*. This recombinant peptide, called Jaburetox-2Ec, carries a V5 epitope and a His tag [15] [14,15] and it displays a potent entomotoxic effect against insects with either cathepsin- or trypsin-based digestive systems. Later on, a recombinant peptide called simply Jaburetox, containing only the His-tagged urease-derived sequence and the same biological properties described for Jaburetox-2Ec was produced [16]. Jaburetox and JBU share several biological properties such as insecticidal activity, neurotoxicity and inhibition of insect diuresis, as well as antifungal effect on filamentous fungi and yeasts [11], suggesting that the JBU region encompassing the peptide sequence accounts for most of its biological activities. High resolution Nuclear Magnetic Resonance, Circular Dichroism, Static and Dynamic Light Scattering were applied to study Jaburetox structural properties revealing that this peptide behaves mostly as an intrinsically disordered protein (IDP) in aqueous solution [17]. The IDP characteristics of Jaburetox could be an important aspect for determining its interaction with liposomes, since it is known that some IDPs may undergo disorder to order transitions in the presence of ligand [18,19].

Jaburetox-2Ec was shown to permeabilize carboxy-fluorescein loaded anionic unilamellar liposomes [20]. Molecular dynamics applied to Jaburetox predicted that its ability to anchor at a polar/non-polar interface is the basis for its membrane permeabilization-promoting effect [20]. Piovesan et al. [21] reported the first direct demonstration of the capacity of JBU and Jaburetox to permeabilize membranes through an ion channel-based mechanism. JBU, Jaburetox and truncated versions of the peptide formed well-resolved, highly cation-selective channels [21]. In that study the region comprising Jaburetox (G222 to I314) in the JBU molecule (total of 841 amino acids) was hypothesized to be the membrane-interacting domain of the protein [21].

Lipid vesicles, commonly referred to as liposomes, are colloidal structures having an aqueous internal core and a membrane formed by phospholipids self-associated in aqueous solution [22–24]. Because of their organization into lipid bilayers, liposomes have been widely used as biological membranes models [25]. The liposomal stability is a key point to their diverse applications in pharmaceutical research and industry as a representative model of cellular membranes [25].

Based on the evidence of an ion-selective pore-formation mechanism employed by JBU to permeabilize phospholipid membranes [21], the present study aims to investigate the interaction of liposomes with both JBU and Jaburetox-2Ec. For that, multilamellar liposomes (PML), consisting of a mixture of lipids characteristic of human platelet membranes were tested with JBU and Jaburetox-2Ec. Their interactions were studied by Small Angle X-ray Scattering (SAXS) and Dynamic Light Scattering (DLS). In addition, the interaction of giant unilamellar vesicles (GUVs) with JBU was studied by Fluorescence Microscopy.

2. Materials and methods

2.1. Materials

The lipids L-α-phosphatidylcholine (PC, >98%), cholesterol (CHOL, >99%), L-α-phosphatidylethanolamine, (PE, >99%), sphingomyelin (SM, >97%), L-α-phosphatidyl-L-serine (PS, >97%), and L-α-phosphatidylinositol (PI, >50%) were purchased as a powder from Sigma-Aldrich, and dissolved in chloroform. Urease type III from *C. ensiformis* (Jack bean) was obtained from

Sigma-Aldrich. The 1,2-dioleoyl-*sn*-glycero-3-phosphoethanolamine-*N*-(Lissamine rhodamine B sulfonyl) (ammonium salt) – (Rhodamine-PE, >99%) was purchased from Avanti Polar Lipids. Triton X-100 was purchased from the InLab Company.

2.2. Urease and Jaburetox preparation

Crystalline Jack bean Urease (type C3, Sigma) was dissolved in and dialyzed against buffer (20 mM sodium phosphate, 1 mM EDTA and 5 mM β-mercaptoethanol pH 7.5), in order to remove salts. JBU solutions (Mw 540.000 Da, 0.75 mg mL^{-1}) were stored at 4 °C. Jaburetox-2Ec expression and purification were carried out as described elsewhere [15]. The recombinant Jaburetox-2Ec comprises 93 amino acid residues derived from JBURE-II sequence, a V-5 epitope of 28 amino acids, and a 6 His-tag, with a total molecular mass of 13.668 kDa and an isoelectric point of 5.30. The disorder propensity of Jaburetox-2Ec was evaluated using algorithms (VLXT, VL3 and VSL2) of the PONDR family (www.pondr.com).

2.3. Liposome preparation

Platelet-like multilamellar liposomes (PML) with the main lipid composition found in human platelets [26] were prepared by applying the reverse phase evaporation method [27,28]. Accordingly, 60 mg of lipids (34.1% PC, 25.8% CHOL, 24.3% PE, 7.7% SM, 6.1% PS and 2% PI, expressed as percent mole) were dissolved in chloroform and dispersed in water by ultra-sound. An organogel was obtained after chloroform evaporation which reverts into a suspension of PML upon addition of water and agitation [28]. The zeta potential of PML in aqueous solution was found to be of -37 ± 3 mV. In interaction experiments, JBU or Jaburetox-2Ec (final concentration 0.5 μM) were added to the aqueous suspension (0.15 M NaCl) containing PML. In order to establish whether the JBU interaction with PML is due to a detergent-like action, we performed control experiments by adding 1% Triton X-100 to PML.

2.4. GUVs preparation

Giant unilamellar vesicles (GUVs) were produced following the electroformation method [28]. Briefly, 10 μL of a lipid mixture solution (1 mg mL^{-1} of lipids consisting of 34.1% PC, 25.8% CHOL, 24.3% PE, 7.7% SM, 6.1% PS, 97%, and 2% PI in chloroform) and 0.5% of Rhodamine-PE (mol mol^{-1}) were spread on an indium tin oxide (ITO)-coated glass slide. After drying the lipid film under vacuum for 30 min, a chamber was formed with a second ITO slide and a Teflon spacer. This chamber was filled with 0.2 M sucrose solution. The osmolarity was measured with an osmometer (Osmomat 030, Gonotec, Berlin, Germany). An alternating electric field was applied across the chamber for 2 h. The amplitude and the frequency of the field were 1 V and 10 Hz, respectively. The obtained GUVs were transferred to an Eppendorf tube. For visualization in the microscope, a solution of 0.2 M glucose was added to the GUVs suspension. Because of the difference in density between glucose and sucrose, the sucrose-containing GUVs settle at the bottom of microscope slides, allowing visualization of the vesicles. For fluorescence microscopy experiments, the JBU solution was first transferred to a glass slide, followed by addition of GUVs. Microscopy images were collected immediately thereafter. The effect of JBU in GUVs was tested at three protein concentrations of 0.01 μM, 0.1 μM and 0.5 μM. At least 10 independent visualization experiments were performed for each JBU concentration.

2.5. Dynamic light scattering

Normalized electric field correlation functions $g_1(t)$, calculated from the intensity autocorrelation functions $g_2(t)$, were analyzed using the algorithm REPES (incorporated in the GENDIST program) which employs the inverse Laplace transformation according to Eq. (1) [29].

$$g_2(t) - 1\beta \left[\int A(\tau) \exp(-t/\tau) d\tau \right]^2$$

where t is the delay time of the correlation function and β is a coefficient accounting for ideal correlation. The relaxation time τ or the relaxation frequency $\Gamma(\tau\text{-}1)$ is associated with a diffusion coefficient D through the relation

$$D = \Gamma/q^2 \tag{2}$$

where q is the scattering vector.

Finally, the hydrodynamic radius (R_h) is derived from the determined value of D using the well-known Stokes-Einstein relation [30]:

$$R_h = \frac{k_B T}{6\pi \eta D}$$

wherein k_B is the Boltzmann constant, T is the absolute temperature and η is the viscosity of the solvent.

Measurements were performed at $25 \pm 0.1\,^\circ$C using a Brookhaven Instruments standard setup (BI200M goniometer, BI9000AT digital correlator) with a vertically polarized Coherent He-Ne laser ($\lambda = 632.8$ nm) as light source. The scattering volume was minimized using a 0.4 mm aperture. The time correlation functions were measured in the multi-τ mode using 224 channels. The samples were filtered through 0.45 nm pore diameter membranes (Millipore) into dust-free vials, which were placed in a cell containing decahydronaphthalene (Aldrich), an index-matching liquid, for the light scattering experiment. The scattered light was analyzed and the values of R_h were obtained at 90°. Measurements were done in triplicate, and results are shown as means ± standard deviations.

2.6. Zeta potential

These analyses are based on the Laser Doppler Velocimetry and the zeta potential (ζ) is deduced from the electrophoretic mobility (U_E) according to the Henry's equation:

$$U_E \frac{2\varepsilon \zeta f(k_a)}{3\eta} \tag{4}$$

where ε is the dielectric constant, η is the viscosity of the medium and $f(k_a)$ is the Henry's function. Considering the Smoluchowski model for particles of 200 nm or more of diameter, $f(k_a) = 1.5$ was assumed [31].

The zeta potential measurements of the particles were performed on a Zetasizer (Malvern Instruments model ZEN3500) with a coherent He-Ne 632.8 nm laser, 4.0 mV as light source. The samples were diluted (0.2% v/v) in 1 mM NaCl and the measurements were conducted in triplicate at room temperature.

2.7. Small angle X-ray scattering

In a Small Angle X-ray Scattering (SAXS) experiment, the number of scattered photons is counted as a function of the scattering angle (θ). In this case, the scattering vector module q is not dependent on the refractive index. The range of q typically available varies from 0.006 to 6 nm^{-1}. For a certain system of scattering particles, the intensity of scattered X-rays $I(q)$ is given by [32]:

$$I(q) = nP(q)S(q) \tag{5}$$

where n is the numeric density of the particles, $P(q)$ refers to the form and size of the particles and is related to the scattering of a simple isolated particle and $S(q)$ comes from interactions between different particles.

The structure factor ($S(q)$) was modeled by the modified Caillé theory (MCT) [33] as given in Eq. (6):

$$S_{MC}(q, N, d, \eta_1, \gamma) = \sum_{N_K = N-2\sigma}^{N+2\sigma} x_K S_{K,MC} \tag{6}$$

where γ is Euler's constant and $S_{k,MC}$ is defined by:

$$S_{K,MC} = N_K + 2 \sum_{m=1}^{N_K+1} (N_K - m) \cos(mqd) \exp - \left[\left(\frac{d}{2\pi} \right)^2 q^2 \eta_1 \gamma \right] (\pi m)^{- \left[\left(\frac{d}{2\pi} \right)^2 q^2 \eta_1 \right]} \tag{7}$$

The fitting parameters considered here were the total number of layers within the scattering domain N, the lamellar repeat distance d, the Caillé parameter η – a measure for bilayer bending fluctuations [34].

The fitting procedure was performed by using the SASfit software which makes use of the least-squares fitting approach to minimize the chi squared (χ^2) parameter. The SASfit software package was developed by J. Kohlbrecher and it is available online [35].

SAXS experiments were performed at the SAXS2 beamline of the Brazilian Synchrotron Light Laboratory (LNLS – Campinas, SP, Brazil). The liquid unfiltered samples were placed in a stainless steel sample holder closed by two mica windows with 25 mm of thickness and kept at 25 °C with an accuracy of ±0.1 °C. An exposure time of about 10 min was required for all samples. The wavelength of the incident beam was 1.488 Å. Isotropic 2D-images were obtained, and corrected by taking into account the detector dark noise and normalized by the sample transmission considering the 360° azimuthal scan. The above procedure has been undertaken using the FIT2D software developed by Hammersley [36].

2.8. Fluorescence microscopy

An inverted TE 200 microscope (Nikon, Japan), equipped with a 60× Water Immersion, 1.2 NA Plan Apo DIC objective was used. A mercury lamp provided the illumination for fluorescence experiments. A fluorescent block with filters Ex. 450–490 nm/BA 520 nm and a 505 nm dichroic mirror was used. Pictures were recorded via a digital camera (NDIAG 1800; Diagnostic Instruments, Sterling Heights, MI) onto the hard disk of a personal computer, with a pixel depth of eight bits.

3. Results

3.1. DLS

In order to study the influence of JBU on PML, their hydrodynamic radii (Rh) were analyzed in the presence of 0.5 μM JBU (final concentration), at 10 min, 30 min and 24 h after exposition to the protein as shown in Fig. 1. In the absence of JBU, PML showed a distribution with one peak only, corresponding to Rh 155 ($\pm$7) nm. After 10 min and 30 min of JBU addition, a two-peak distribution was observed, corresponding to Rh 9 ($\pm$1) nm and 141 ($\pm$6) nm, respectively. The smaller particles correspond to JBU molecules in solution, considering the REPES analysis of a protein solution that
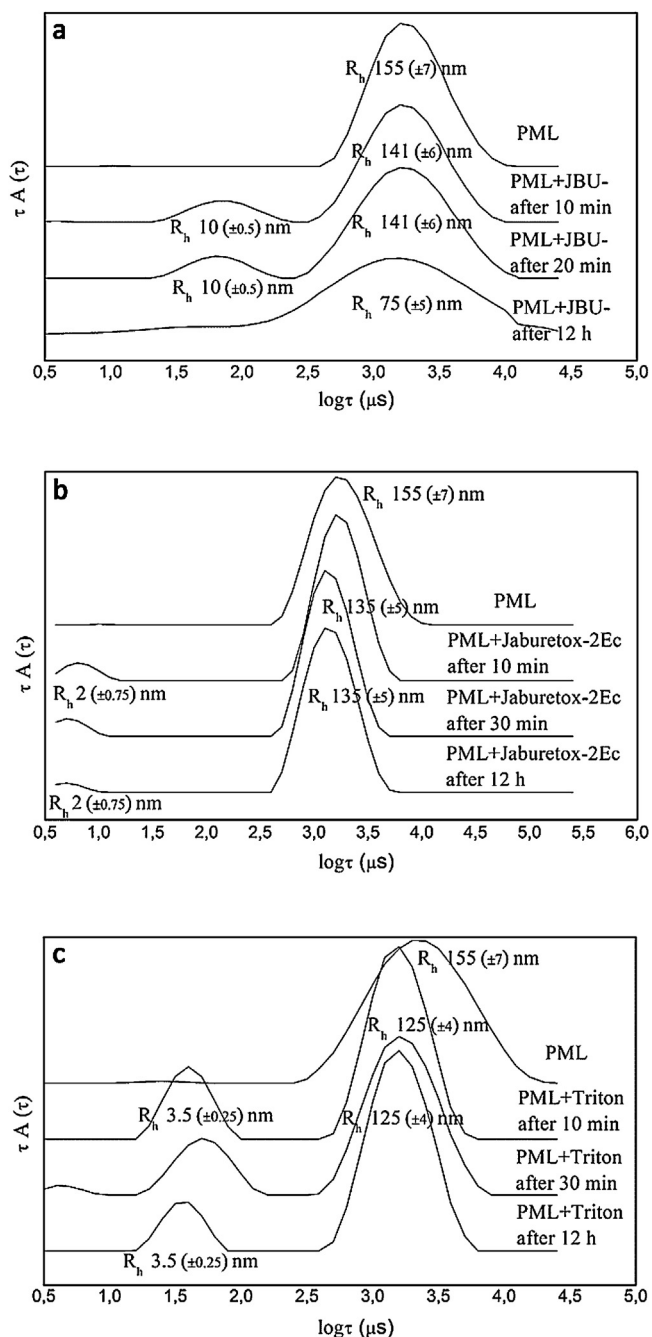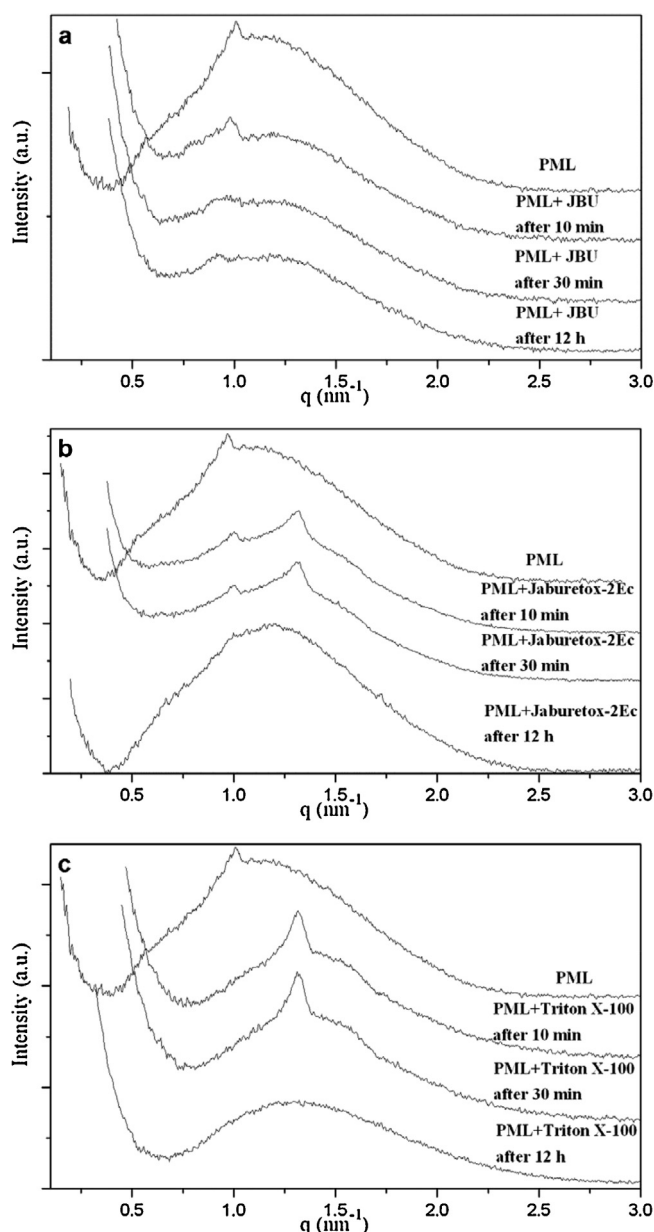
Fig. 1. Distribution of relaxation times obtained by DLS for platelet-like multilamellar liposomes (PML) in the absence and after 10 min, 30 min and 12 h in the presence of (a) 0.5 μM JBU; (b) 0.5 μM Jaburetox-2Ec; (c) 1% Triton X-100. A typical result for each compound out of a triplicate is shown.

Fig. 2. SAXS curves of platelet-like multilamellar liposomes (PML) in the absence and after 10 min, 30 min and 12 h in the presence of (a) 0.5 μM JBU: (b) 0.5 μM Jaburetox; (c) 1% Triton X-100. A typical result for each compound out of a triplicate is shown.

yields Rh 10 ($\pm$0.5) nm. This Rh value is close to the 7 nm value found for JBU by Follmer et al., 2004 [37].

The R_h value of 141 nm is related to PMLs upon interaction with JBU. After one day, only one large and broad peak was observed (Fig. 1a), indicating that all JBU molecules interacted with PML, clearing the solution of any free protein.

Interaction of Jaburetox-2Ec with PMLs was also studied by following changes of R_h, using the same parameters as used for JBU. After exposition of PMLs for 10 min, 30 min and 24 h to 0.5 μM Jaburetox-2Ec, two peaks appeared in the distribution of relaxation times, corresponding to R_h of 2 ($\pm$0.75) nm and 135 ($\pm$5) nm, respectively (Fig. 1b). The smaller particles (R_h 2 nm)

correspond to free Jaburetox-2Ec peptides in solution. Indeed, according to Lopes et al. [17], Jaburetox presents a Rh of 2.7 nm in 50 mM sodium phosphate buffer, pH 7.5, 1 mM EDTA, 1 mM TCEP (*tris*(2-carboxyethyl)phosphine) [17]. The larger particles (130 nm) reflected the interaction of Jaburetox-2Ec with the PMLs.

In order to verify whether the interactions of JBU or Jaburetox-2Ec with PML were similar to the detergent action of Triton-X-100, we performed a control sample of PML in the presence of 1% Triton X-100. Fig. 1c shows the distribution of relaxation times of PML in the presence and absence of Triton X-100. After 10 min, 30 min and 24 h of the addition of Triton X-100, the presence of two populations of particles, one with R_h 3.5 ($\pm$0.25) nm and another with R_h 125 ($\pm$4) nm, were observed. The smaller population could be ascribed to mixed micelles (lipid/Triton X-100) or Triton X-100 micelles (R_h = 3.5), as determined by REPES [38]. The larger population corresponds to vesicles upon interaction with Triton X-100.

Table 1
Form and structure (when present) factor parameters of PML in the presence of 0.5 μM JBU, 0.5 μM Jaburetox-2Ec, or 1% Triton X-100 after 10 min and 12 h of exposition. Values of χ^2 were <5 for all fits obtained.

Sample	Form Factor[a]		Structure Factor[b]		
	t_h (nm)	t_t (nm)	d (nm)	η	N
PML	1.41	2.29	6.23	0.96	14
PML + JBU – 10 min	1.40	2.72	6.48	0.64	7
PML + JBU – 12 h	1.40	2.37	6.98	0.53	7
PML + Jaburetox-2Ec – 10 min	1.38	2.75	6.32/4.72[b]	0.96/0.85[2]	14/9[b]
PML + Jaburetox-2Ec – 12 h	1.48	2.40	–	–	–
PML + Triton X-100–10 min	1.52	2.24	4.75	0.90	10
PML + Triton X-100–12 h	1.40	2.25	–	–	–

[a] Parameters obtained from fitting theoretical curves to experimental data.
[b] Structure factor parameters related to first peak/second peak, respectively. In the table, t_h is the thickness of outer part of bilayer, t_t is the thickness of inner part of bilayer, d is the lamellar repeat distance, η is the Caillé parameter and N is the number of layers within the scattering domain. Values of χ^2 were <5 for all fits obtained.

The distribution with two peaks seen after 10 min persisted until 24 h of observation.

3.2. SAXS

Fig. 2a shows SAXS curves obtained for PML before and after 10 min, 30 min, and 12 h of addition of JBU at 0.5 μM final concentration. A progressive decrease in intensity of the Bragg peak (q = 1.00 nm^{-1}) was observed up to 12 h, at which point the peak is effectively undistinguishable from the form factor, indicating that JBU caused disorder in the PML membrane, changing the liposome organization mostly to a unilamellar state.

Similarly, SAXS analyses were performed for the interaction of Jaburetox-2Ec with PMLs before and after 10 min, 30 min and 12 h of addition of 0.5 μM Jaburetox-2Ec (Fig. 2b). The SAXS curve of Jaburetox-2Ec plus PML showed two superimposed Bragg peaks on a broad scattered background. The position of the Bragg peak (q = 1.00 nm^{-1}) found in the SAXS for PML alone was not affected by Jaburetox-2Ec interaction. However, the appearance of a second Bragg peak observed at $q = 1.33$ nm^{-1} indicated an interaction of Jaburetox-2Ec with lipids. This peak reflects the partially perturbed hydrocarbon side chains, suggesting an interaction of Jaburetox-2Ec with some fraction of the lipids. As it was seen for JBU, the Bragg peaks disappeared after 12 h, indicating that at this time mostly unilamellar liposomes remained in the sample.

2c shows PML SAXS curves in the absence or presence of 1% Triton X-100, after 10 min, 30 min, and 12 h. The presence of Triton X-100 causes a shift in the Bragg peak of q = 1.0 nm^{-1} to q = 1.33 nm^{-1} with an increase in its intensity. In contrast to the liposome interaction with Jaburetox-2Ec, no significant sign of a peak at q = 1.0 nm^{-1} remained after 12 h. The Bragg peak is not observed because only unilamellar vesicles are present in the suspension, similar to what was observed for PMLs after 12 h in the presence of JBU or Jaburetox-2Ec. Supplementary Figs. S4, S5 e S6 shows the superimposed SAXS curves of the PML before and after 12 h of interaction with JBU, Jaburetox-2Ec and Triton X-100. Experiments carried out with PMLs exposed to 0.1 μM JBU and 0.1 μM of Jaburetox-2Ec showed the same SAXS profile as with 0.5 μM ones (Supplementary Fig. S7). The experimental margin of error for all q values is of ±0.01 nm^{-1} or less.

Theoretical fitting of the Jaburetox-2EC SAXS curve was best achieved by combining two structure factor curves (Fig. 3). The first one had parameters very similar to those of the pure PMLs in solution, while the second one presented a considerably lower value for lamellar repeat distance (d), as well as reduced Caillé parameter (η) (Table 1). The SAXS profile remained largely identical for the

measurements in the first 40 min, but after 12 h both peaks disappeared, as observed in JBU experiment

Fitting of the interaction of the vesicles with Triton X-100 showed a decrease in lamellar repeat distance, similar to that indicated by the second peak of the Jaburetox-2Ec interaction. In contrast, unlike both JBU and Jaburetox-2Ec, Triton X-100 did not cause a significant decrease of the Caillé parameter (Table 1).

According to data summarized in Table 1, upon interaction with JBU there was a slight increase in the lamellar repeat distance (d) of PML after 10 min and 12 h. On the other hand, the number of lamellar repeat (N) and the Caillé parameter (η) decreased following the interaction of JBU with the PML membrane. The reduction of the Caillé parameter indicates that JBU caused an increase in the rigidity of the bilayer lipid [34], reflecting the insertion of the protein into the bilayer.

In the case of the liposome's interaction with Jaburetox-2Ec, a considerable decrease of the lamellar repeat distance is seen for the second peak. A reduction of the Caillé parameter, although not as large as in the JBU interaction, is also observed and interpreted here as a result of the insertion of the smallest peptide into the bilayer. A decrease in the number of lamellar repeat (N) was verified as well.

3.3. Fluorescence microscopy

The effect of JBU on GUVs was tested for three protein concentrations (0.01, 0.1 and 0.5 μM), using a fluorescence microscopy technique. At the lowest JBU concentration (0.01 μM) perturbations of the membrane were seen, with the formation of tethers (long, thin protuberances originating from the membrane [39]) inside or outside the GUVs (Fig. 4a). This phenomenon occurs within few minutes after the transfer of GUVs into the JBU solution, but not all vesicles were affected. At concentration of 0.1 μM of JBU (Fig. 4b), besides the formation of tethers, severe deformations and budding of the membrane were seen. Fig. 4b shows a sequence of GUV deformation events observed few minutes after exposition to JBU at 0.5 μM; besides the membrane perturbation, most GUVs developed outside threads (Fig. 4c). After 24 h of the first analysis, GUVs samples exposed to JBU, as well as control GUVs in the absence of JBU, were analyzed again. All samples containing JBU presented a low number of GUVs, with sizes smaller than 10 μm, while control GUVs remained mostly unchanged. Over the time, with most JBU molecules inserted into GUV membranes, the membrane permeability was altered, facilitating the influx of the smaller glucose molecules (r = 0.44 nm) more than the outflux of larger internal sucrose molecules (rs = 0.55 nm), thus causing water's movement into the vesicle to maintain the osmotic equilibrium [40]. This led to rupture of the vesicles permeabilized by JBU, while control GUVs remained intact.

4. Discussion

In this work, we investigated the interaction of JBU and its derived peptide, Jaburetox-2Ec, with PML and its effect on the vesicles' R_h. Both urease-derived peptides, Jaburetox and Jaburetox-2Ec (containing a V5 epitope) present the same biological properties and are equipotent in terms of molar concentration [16]. Here we employed Jaburetox-2Ec due to its higher production yield and its increased stability when in solution. DLS analysis showed that interaction with both JBU and Jaburetox-2Ec caused a slight R_h reduction in the liposomes, while Triton X-100 led to a more pronounced Rh reduction. Triton X-100 did not destroy PML completely under our experimental time lapse, reflecting the stable multilamellar nature of the liposomes. In contrast, in tests with unilamellar liposomes, both here as well as in [38], a complete solubilization of unilamellar liposomes after exposition to 1%
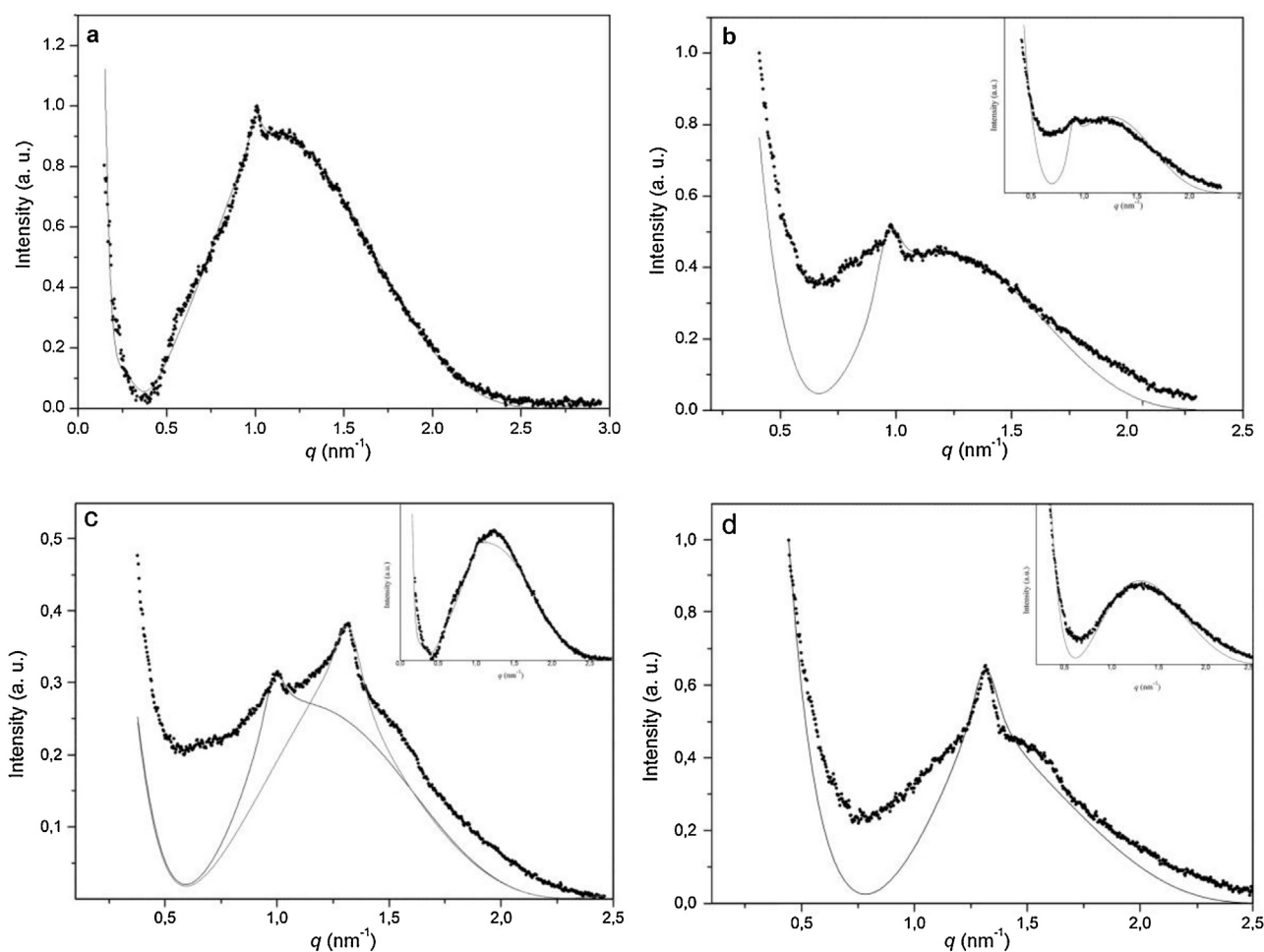
Fig. 3. Best fitting of SAXS curve to (a) PML, (b) PML in the presence of 0.5 μM JBU after 10 min, (c) PML in the presence of 0.5 μM Jaburetox-2Ec after 10 min, and d) PML in the presence of 1% Triton X-100 after 10 min. The insets in each graphic show the results for the same samples after 12 h. A typical result for each compound out of a triplicate is shown. Parameters obtained to the form and structure factor are listed in Table 1.

Triton X-100 was observed, showing that the number of lamellae is important in the mode of action of Triton X-100 [38].

Although multilamellar liposomes are not widely used to evaluate the cellular interactions of proteins and peptides, using them in this work allows the analysis of the Bragg peak, a typical variable of multilamellar structures, which provided important parameters that revealed the JBU and Jaburetox-2Ec mode of interaction with PML [40]. Liposomes with a lipid composition typical of human platelets membrane were used in this study because of the well-known property of JBU and other plant and bacterial ureases to activate and aggregate blood platelets [41,42].

Other studies of peptides interaction with multilamellar liposomes using similar techniques were reported. Willumeit et al. [43] developed an antimicrobial peptide named NK-2 that binds to anionic phosphatidylglycerol liposomes, causing a thinning of the membrane, due to electrostatic and hydrophobic interactions. Pabst et al. [44] used X-ray diffraction to observe the perturbation of saturated acyl chain phosphatidylglycerol bilayers caused by the antimicrobial peptide peptidyl-glycyl-leucinecarboxyamide (PGLa), that is dependent on the length of the hydrocarbon chain.

As indicated by results obtained by SAXS, JBU caused a slight increase in PML's lamellar repeat distance (d) both after 10 min and 12 h, while Triton X-100 led to a reduction of the lamellar repeat distance after 10 min, and disappearance of the peak after 12 h. Interaction with Jaburetox-2Ec, however, led to the formation of a second Bragg peak with a significant smaller lamellar repeat distance (d), while still retaining the characteristic peak of the original

PMLs. In the present study, the number of lamellar repeat (N) was reduced in all cases, suggesting that JBU, Jaburetox-2Ec, and Triton X-100 caused a decrease of PML size. The presence of JBU or Jaburetox-2Ec promoted a reduction in the Caillé parameter (η) – more significant in the former – indicating higher membrane rigidity due to the protein/peptide insertion into the lipid membrane(s). The higher increase in rigidity observed for JBU likely reflects its larger size comparing with Jaburetox-2Ec.

Hence, we concluded that JBU interacts with PML by inserting itself into the membrane, as indicated by the disappearance of the free JBU peak, the observed membrane disorder as well as a breakdown of lamellar order in the liposomes, reflected by the reduction of the Bragg peak after 12 h (Fig. 3b inset). Moreover, a decrease of the form factor in the SAXS curve of liposomes after 12 h in presence of JBU as compared to the pure liposome sample was observed (Supplementary material Fig. S4). The decrease of 0.6 in the absolute intensity value in the curve indicates a loss of lamellae by this same factor due to interaction with JBU. No great changes of the form factor q values were seen after 12 h. The estimated total mass of JBU in the sample was 2.7×10^{-3} g, compared to an estimated mass of 3.0×10^{-4} g of lipids. The insertion of JBU into the liposome membrane might cause a removal or redistribution of lipids from the membrane through the formation of filaments and/or induction of a different lamellar organization. This insertion process is possibly centered around the pepcanatox (which is equivalent to Jaburetox-2Ec) region of the JBU molecule (Fig. 5). Crystallographic studies of the JBU molecule showed that
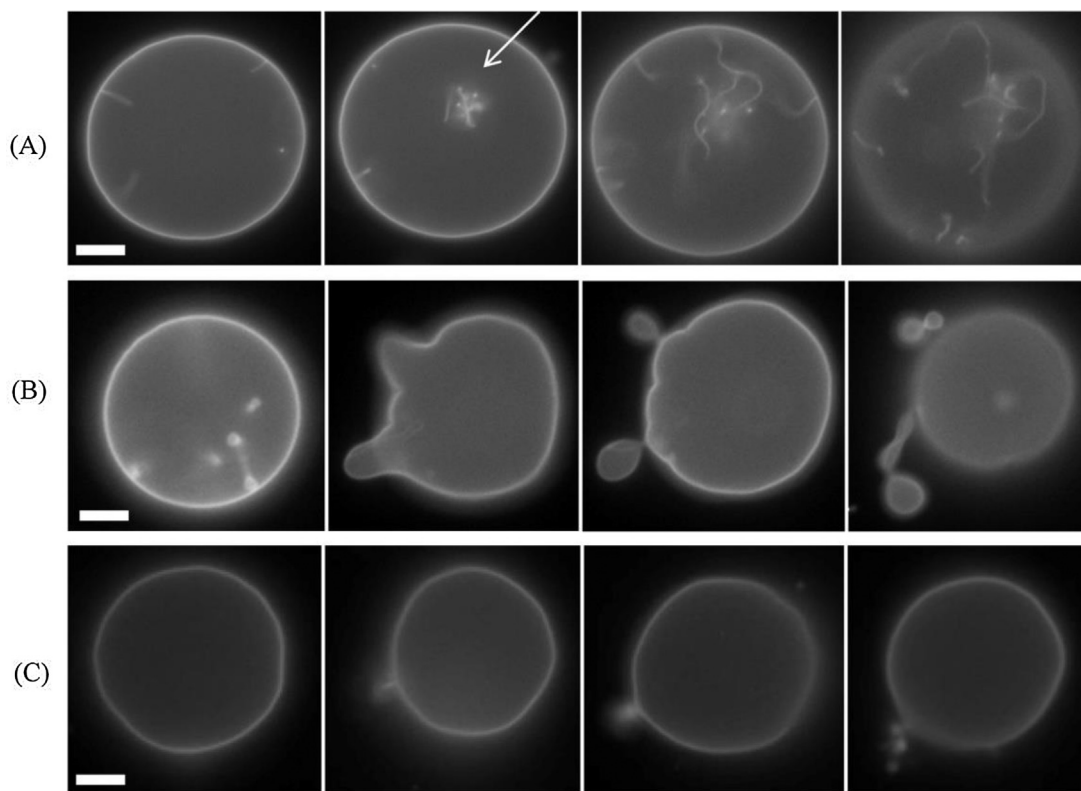
Fig. 4. Effects of JBU on GUVs. (A) 0.01 μM JBU, 10 min exposition. The arrows show tethers inside the vesicles. (B) 0.1 μM JBU, 10 min exposition. Membrane budding and deformations in GUVs are seen in the presence of the protein. (C) 0.5 μM JBU. Tethers are seen outside the GUVs. A typical result for each JBU concentration (N = 10) is shown. Scale bars span 10 μm.

this region is well exposed at its surface, consisting of a big loop with few structural elements, among which a prominent beta-hairpin and small amphiphilic helices (Fig. 6a) that could potentially mediate the interaction of the protein with cell membranes [3]. One can hypothesize that the large size of the JBU molecule causes steric hindrance to its clustering together as to effectively disrupt the bilayer structure, as well as preventing the molecule to traverse through any pore formed on the external bilayer, or to affect the internal ones.

On the other hand, the smaller Jaburetox-2Ec peptide presents the same hydrophilic and hydrophobic portions seen in Jaburetox [45]. When in solution, Jaburetox behaves as an intrinsically disordered polypeptide (Fig. 6b), a class of molecules prone to interaction with different ligands including lipids [17–19]. Fig. 6c shows the intrinsic disordered nature of Jaburetox-2Ec using disorder predictor algorithms of the PONDR family. The N-terminal region of Jaburetox-2Ec probably is the region that interacts with lipids, as disordered-based binding sites were predicted in this region of Jaburetox [17]. Thus, it is conceivable that Jaburetox peptide(s) could anchor to the hydrophobic core of the membrane bilayer through its hydrophobic groups, and subsequently insert and cluster itself in the membrane. The smaller size of Jaburetox-2Ec could also allow the peptide to cross any membrane pores and affect the internal bilayers, causing drastic changes in the PML structure as seen in the SAXS analysis, which may be representative of a new lamellar structure [46]. Also, unlike the JBU, the larger number of the smaller Jaburetox-2Ec molecules in solution led to a portion of the peptide remaining free in the aqueous solution after 12 h, despite the estimated total mass of Jaburetox-2Ec in the sample (6.8×10^{-5} g) being one order of magnitude smaller than the mass of lipids. The decrease of the form factor of liposomes after 12 h in presence of Jaburetox (Fig. 3c inset) is smaller than the decrease

seen for JBU (Supplementary material Fig. S5). This small decrease might indicate that the liposomes membranes did not lose a large amount of lipids upon interaction with the polypeptides, although becoming a little thinner, as indicated by the decrease in the d parameter. The loss of the structure factor peak after 12 h, however, indicates that these remaining bilayers have lost their original multilamellar arrangement [47].

Triton X-100 interacts with PML by "removing" lipids of its most external layers, with the formation of a new population of micelles composed by Triton X-100 and lipids, leading to progressive decrease of lamellar repeat distance and Rh, resulting 12 h thereafter in only unilamellar PML detectable in the suspension. Additionally, a decrease of 0.6 was seen in the form factor values of the Triton X-100-(Fig. 3d inset) and of JBU-treated (Supplementary material Fig. S6) liposomes after 12 h. Moreover, a displacement of the whole form factor to a higher range of q values was also observed. The detergent Triton X-100, which is present in the sample in a mass ratio 300-fold higher than the lipids, destroyed the lamellar structure of the liposomes in 12 h. These results point to differences in the mode of interaction of JBU, Jaburetox-2Ec, and Triton X-100 with the PML, where JBU and Triton X-100 cause a general disorder and destruction of the liposomes and Jaburetox-2Ec causes a change in its structural organization, at least part of its lipid bilayer.

The zeta potential of PML in aqueous solution was -37 ± 3 mV, reflecting its colloidal stability [48]. This negative potential is due to the presence of anionic phospholipids (PS and PI) in the composition of the PMLs. Barros et al. [20] reported the ability of Jaburetox-2Ec to permeabilize anionic lipid bilayers without causing rupture of the vesicles. In this study, Jaburetox-2Ec in solution (pH 7.5) was above its isoelectric point (IP), thus presenting negative charge. JBU in solution (pH 7.5) was also above its IP (4.5) and
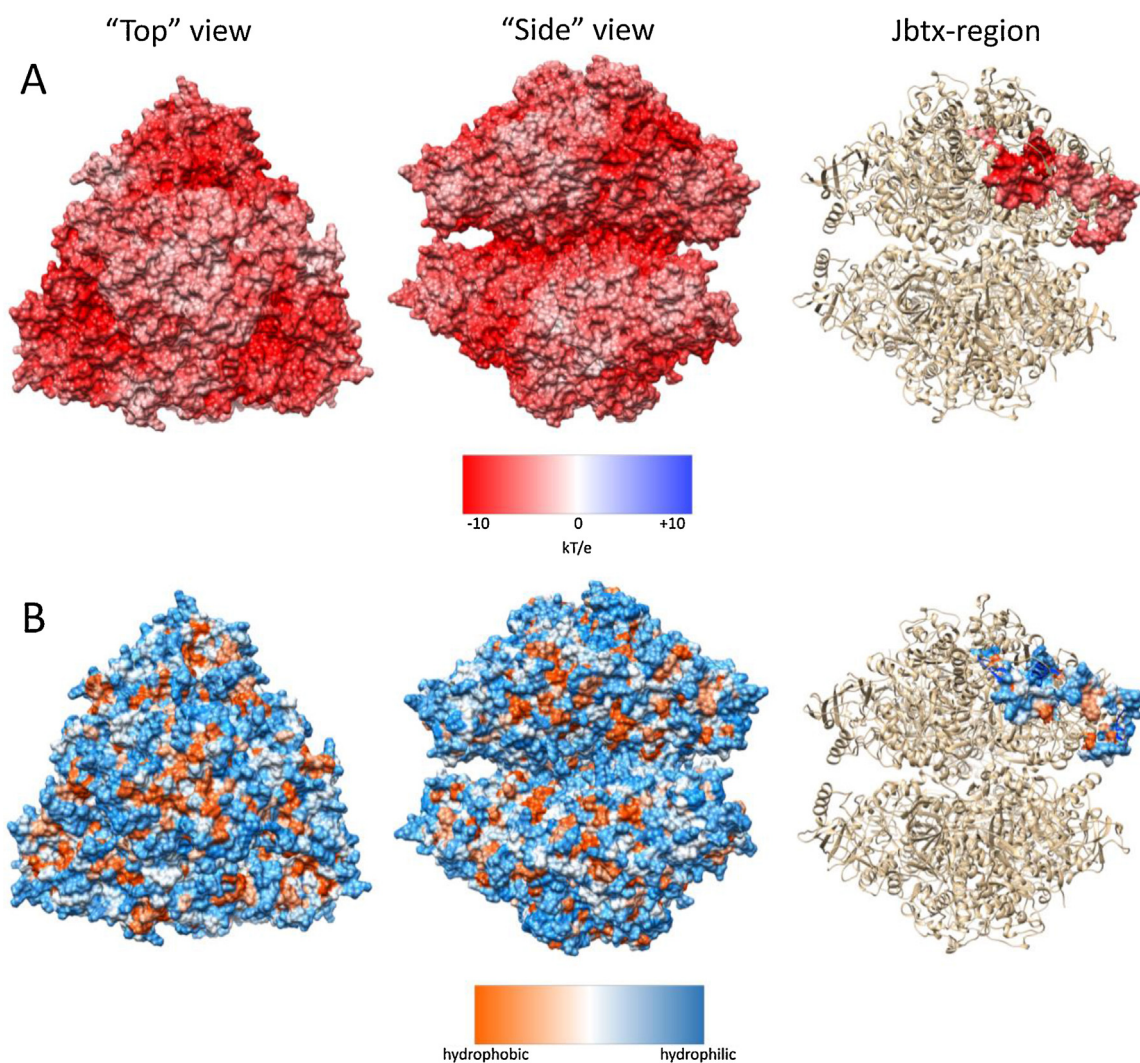
Fig. 5. Surface properties of JBU hexamer (reference structure PDB id 3LA4 [3]). The location of the pepcanatox/Jaburetox sequence in one of the monomers shown at the right side of each panel. (A) Electrostatic properties of JBU, colored according to the electrostatic potential (red, negative; blue, positive). (B) Hydrophobicity properties of JBU, colored according to the Kyte-Doolittle scale (orange, hydrophobic; light blue, hydrophilic). "Top" and "side" views of the oligomer are relative rather than absolute representations; the Jbtx-region of one monomer is represented in the same orientation as the "side" view. Image generated with UCSF Chimera [55] using APBS tools [56] and Kyte-Doolittle scale [57]. (For interpretation of the references to color in this figure legend, the reader is referred to the web version of this article.)
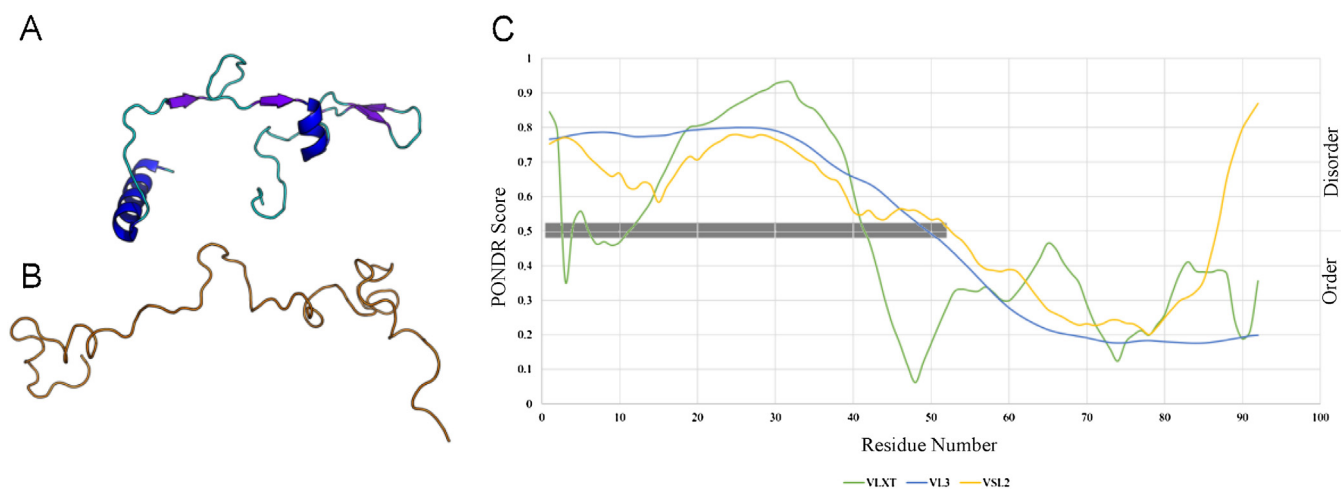
Fig. 6. Jaburetox-2Ec and Jaburetox disordered features. (A) Crystal-derived Jaburetox structure, from entire JBU (PDB ID 3LA4, [3]); (B) NMR-derived Jaburetox structure (PDB ID 2MM8, [17]); (C) Structural disorder prediction for Jaburetox-2Ec, according to PONDR software [58]. A and B depicted to scale, N-terminus to the left. The grey bar indicates the most disordered region of Jaburetox-2Ec.

negatively charged. Thus, it seems that hydrophilic/hydrophobic interactions are more important than the electrostatic attraction regarding the insertion of JBU into the liposome membrane. As observed in Fig. 5, JBU has a predominant negative electrostatic potential and the majority of its surface is hydrophilic. The region of JBU that encompasses the pepcanatox sequence – the Jaburetox-2Ec "domain" of the protein – is well exposed on its surface. Due to its amphiphilic nature and flexibility, we suggest that this Jaburetox "domain" can insert itself into lipid bilayer in order to drive the interaction of JBU with the liposome's membrane.

We also studied the interaction of JBU with GUVs by means of fluorescence microscopy. GUVs are well accepted models of biological membranes with sizes similar to living cells (5–50 µm) and are easily observed under an optical microscope. Thus, GUVs have been used in studies of membrane properties and interaction with biological molecules [49,50]. The data on interaction of GUVs with JBU showed a concentration-dependent effect. At lower concentrations JBU (0.01–0.1 µM) caused formation of tethers inside and outside GUVs but their membranes remained impermeable to glucose; while after 12 h of higher concentrations, JBU (0.5 µM) caused lysis of the vesicles due to altered permeability of their membranes. The effects of JBU on the multilamellar lipid vesicles reached a "plateau" after 12 h, when the vesicles were found mostly in a unilamellar state due to the interaction with the protein.

Worth mentioning is that the concentrations of JBU tested on GUVs are within the range in which it promotes effects on a variety of cellular models [51,52], and the protein is not cytolytic or cytotoxic at these same doses, nor does it display any direct or indirect phospholipase activity. [8,53].

Mally et al. [39] investigated the interaction between the pore-forming peptide melittin and GUVs by micromanipulation and direct optical observation of vesicles. They observed a dose-dependent response for melittin ranging from slight perturbation of the membrane to disintegration of the vesicle. A model for melittin-vesicle interaction was proposed based on transmembrane positioning and dimerization of melittin [39]. Sanchez et al. [54] described the interaction of *Crotalus atrox*-secreted phospholipase A2 (sPLA2) with GUVs composed of single and binary phospholipid mixtures, as visualized through two-photon excitation fluorescent microscopy. They observed that, regardless of their lipid composition, all GUVs were reduced in size as sPLA2-dependent lipid hydrolysis proceeded.

5. Conclusion

In this work we studied the interaction of JBU and Jaburetox-2Ec with liposomes consisting of a mixture of lipids characteristic of human platelet membranes. Our results indicated that JBU interacts with PML by inserting its Jaburetox "domain" into the liposome, thereby causing membrane perturbation and disorder. However, this interaction is different than a simple detergent-like action as observed for Triton X-100. On the other hand, the intrinsically disordered Jaburetox-2Ec peptide probably anchors itself within the hydrophobic core of the membrane bilayer with subsequent insertion, affecting the internal bilayers and causing more drastic changes in the PML membrane than JBU. These results shed light on the often proposed, but biophysically elusive, property of ureases and its derived peptides to interact with biological membranes.

Acknowledgements

Appendix A. Supplementary data

Supplementary data associated with this article can be found, in the online version, at http://dx.doi.org/10.1016/j.colsurfb.2016.05.063.

References

[1] N.E. Dixon, J.A. Hinds, A.K. Fihelly, C. Gazzola, D.J. Winzor, R.L. Blakeley, B. Zerner, Jack bean urease (EC 3.5.1.5). IV. The molecular size and the mechanism of inhibition by hydroxamic acids. Spectrophotometric titration of enzymes with reversible inhibitors, Can. J. Biochem. 58 (1980) 1323.

[2] J.B. Sumner, The isolation and crystallization of the enzyme urease, J. Biol. Chem. 69 (1926) 435.

[3] A. Balasubramanian, K. Ponnuraj, Crystal structure of the first plant urease from jack bean: 83 years of journey from its first crystal to molecular structure, J. Mol. Biol. 400 (2010) 274.

[4] M. Hirai, R. Kawai-Hirai, T. Hirai, T. Ueki, Structural change of jack bean urease induced by addition surfactants studied with synchrotron-radiation small-angle X-ray scattering, Eur. J. Biochem. 215 (1993) 55.

[5] C. Follmer, G.B. Barcellos, R.B. Zingali, O.L. Machado, E.W. Alves, C. Barja-Fidalgo, J.A. Guimarães, C.R. Carlini, Canatoxin, a toxic protein from jack beans (*Canavalia ensiformis*), is a variant form of urease (EC 3.5.1.5): biological effects of urease independent of its ureolytic activity, Biochem. J. 360 (2001) 217.

[6] F. Mulinari, A.B. Becker-Ritt, D.R. Demartini, R. Ligabue-Braun, F. Stanisçuaski, H. Verli, R.R. Fragoso, E.K. Schroeder, C.R. Carlini, M.F. Grossi-de-Sá, Characterization of JBURE-IIb isoform of *Canavalia ensiformis* (L.) DC urease, Biochim. Biophys. Acta 1814 (2011) 1758.

[7] C.R. Carlini, A.E.A. Oliveira, P. Azambuja, J. Xavier-Filho, M.A. Wells, Biological effects of canatoxin in different insect models: evidence for a proteolytic activation of the toxin by insect cathepsinlike enzymes, J. Econ. Entomol. 90 (1997) 340.

[8] C.R. Carlini, J.A. Guimarães, J.M.C. Ribeiro, Platelet release reaction and aggregation induced by canatoxin, a convulsant protein: evidence for the involvement of the platelet lipoxygenase pathway, Br. J. Pharmacol. 84 (1985) 551.

[9] C.F. Benjamin, C.R. Carlini, C. Barja-Fidalgo, Pharmacological characterization of rat paw edema induced by canatoxin, the toxic protein from *Canavalia ensiformis* (Jack bean) seeds, Toxicon 30 (1992) 879.

[10] A.B. Becker-Ritt, A.H.S. Martinelli, S. Mitidieri, V. Feder, G.E. Wassermann, L. Santi, M.H. Vainstein, J.T.A. Oliveira, L.M. Fiuza, G. Pasquali, C.R. Carlini, Antifungal activity of plant and bacterial ureases, Toxicon 50 (2007) 971.

[11] C.R. Carlini, R. Ligabue-Braun, Ureases as multifunctional toxic proteins: a review, Toxicon 110 (2016) 90–109.

[12] C.T. Ferreira-DaSilva, M.E. Gombarovits, H. Masuda, C.M. Oliveira, C.R. Carlini, Proteolytic activation of canatoxin a plant toxic protein, by insect cathepsin-like enzymes, Arch. Insect Biochem. Physiol. 44 (2000) 162–171.

[13] A.R. Piovesan, F. Stanisçuaski, J. Marco-Salvadori, R. Real-Guerra, M.S. Defferrari, C.R. Carlini, Stage-specific gut proteinases of the cotton stainer bug *Dysdercus peruvianus*: role in the release of entomotoxic peptides from *Canavalia ensiformis* urease, Insect Biochem. Mol. Biol. 38 (2008) 1023.

[14] M.S. Defferrari, D.R. Demartini, T.B. Marcelino, P.M. Pinto, C.R. Carlini, Insecticidal effect of *Canavalia ensiformis* major urease on nymphs of the milkweed bug *Oncopeltus fasciatus* and characterization of digestive peptidases, Insect Biochem. Mol. Biol. 41 (2011) 388.

[15] F. Mulinari, F. Stanisçuaski, L.R. Bertholdo-Vargas, M. Postal, O.B. Oliveira-Neto, D.J. Rigden, M.F. Grossi-de-Sá, Jaburetox-2Ec: an insecticidal peptide derived from an isoform of urease from the plant *Canavalia ensiformis*, Peptides 28 (2007) 2042.

[16] M. Postal, A.H.S. Martinelli, A.B. Becker-Ritt, R. Ligabue-Braun, D.R. Demartini, S.F.F. Ribeiro, G. Pasquali, V.M. Gomes, C.R. Carlini, Antifungal properties of *Canavalia ensiformis* urease and derived peptides, Peptides 38 (2012) 22.

[17] F.C. Lopes, O. Dobrovolska, R. Real-Guerra, V. Broll, B. Zambelli, F. Musiani, V.N. Uversky, C.R. Carlini, S. Ciurli, Pliable natural biocide: jaburetox is an intrinsically disordered insecticidal and fungicidal polypeptide derived from jack bean urease, FEBS J. 282 (2015) 1043.

[18] V.N. Uversky, A decade and a half of protein intrinsic disorder: biology still waits for physics, Protein Sci. 22 (2013) 693.

[19] P. Tompa, Intrinsically disordered proteins: a 10-year recap, Trends Biochem. Sci. 37 (2012) 509.

[20] P.R. Barros, H. Stassen, M.S. Freitas, C.R. Carlini, M.A.C. Nascimento, C. Follmer, Membrane-disruptive properties of the bioinsecticide Jaburetox-2Ec: implications to the mechanism of the action of insecticidal peptides derived from ureases, Biochim. Biophys. Acta 1794 (2009) 1848.

[21] A.R. Piovesan, A.H.S. Martinelli, R. Ligabue-Braun, J.-L. Schwartz, C.R. Carlini, *Canavalia ensiformis* urease Jaburetox and derived peptides form ion channels in planar lipid bilayers, Arch. Biochem. Biophys. 547 (2014) 6.

[22] O. Mertins, M.B. Cardoso, A.R. Pohlmann, N.P. da Silveira, Structural evaluation of phospholipidic nanovesicles containing small amounts of chitosan, J. Nanosci. Nanotechnol. 6 (2006) 2425.

[23] D.D. Lasic, Novel applications of liposomes, Trends Biotechnol. 16 (1998) 307.

[24] D.D. Lasic, D. Papahadjopoulos, Liposomes revisited, Science 267 (1995) 1275.

[25] E. Casals, A.M.a. Galán, G. Escolar, M. Gallardo, J. Estelrich, Physical stability of liposomes bearing hemostatic activity, Chem. Phys. Lipids 125 (2003) 139.

[26] F. Szoka, D. Papahadjopoulos, Procedure for preparation of liposomes with large internal aqueous space and high capture by reverse-phase evaporation, Proc. Natl. Acad. Sci. U. S. A. 75 (1978) 4194.

[27] O. Mertins, A.R. Pohlmann, N.P. da Silveira, Production of soybean phosphatidylcholine–chitosan nanovesicles by reverse phase evaporation: a step by step study, Chem. Phys. Lipids 138 (2005) 29.

[28] M.I. Angelova, D.S. Dimitrov, Liposome electroformation, Faraday Discuss. Chem. Soc. 81 (1986) 303.

[29] J. Jakes, Regularized positive exponential sum (REPES) program – a way of inverting laplace transform data obtained by dynamic light scattering, Collect. Czech. Chem. Commun. 60 (1995) 1781.

[30] R. Pecora, B.J. Berne, Dynamic Light Scattering With Applications to Chemistry Biology and Phisics, Dover Publications, New York, 2000.

[31] O. Mertins, P.H. Schneider, A.R. Pohlmann, N.P. da Silveira, Interaction between phospholipids bilayer and chitosan in liposomes investigated by 31P NMR spectroscopy, Colloids Surf. B Biointerfaces 75 (2010) 294.

[32] A.F. Craievich, Synchrotron SAXS studies of nanostructured materials and colloidal solutions: a review, Mater. Res. 5 (2002) 1.

[33] R. Zhang, R.M. Suter, J.F. Nagle, Theory of the structure factor of lipid bilayers, Phys. Rev. E 50 (1994) 5047.

[34] R. Zhang, W. Sun, S. Tristram-Nagle, R.L. Headrick, R.M. Suter, J.F. Nagle, Critical fluctuations in membranes, Phys. Rev. Lett. 74 (1995) 2832.

[35] J. Kohlbrecher, SASfit Software package for fitting small-angle scatteringcurves. http://kur.web.psi.ch/sans1/SANSSoft/sasfit html (2011).

[36] A. Hammersley, Scientific software FIT2D http://www.esrf.eu/computing/scientific/FIT2D/ (2009).

[37] C. Follmer, F.V. Pereira, N.P. da Silveira, C.R. Carlini, Jack bean urease (EC 3.5.1.5) aggregation monitored by dynamic and static light scattering, Biophys. Chem. 111 (2004) 79.

[38] O. López, A. de la Maza, L. Coderch, C. López-Iglesias, E. Wehrli, J.L. Parra, Direct formation of mixed micelles in the solubilization of phospholipid liposomes by Triton X-100, FEBS Lett. 426 (1998) 314.

[39] M. Mally, J. Majhenc, S. Svetina, B. Žekš, The response of giant phospholipid vesicles to pore-forming peptide melittin, Biochim. Biophys. Acta 1768 (2007) 1179.

[40] J.A. Bouwstra, G.S. Gooris, W. Bras, H. Talsma, Small angle X-ray scattering: possibilities and limitations in characterization of vesicles, Chem. Phys. Lipids 64 (1993) 83.

[41] D. Olivera-Severo, G.E. Wassermann, C.R. Carlini, Ureases display biological effects independent of enzymatic activity: is there a connection to diseases caused by urease-producing bacteria? Braz. J. Med. Biol. Res. 39 (2006) 851.

[42] G.E. Wassermann, D. Olivera-Severo, A.F. Uberti, C.R. Carlini, Helicobacter pylori urease activates blood platelets through a lipoxygenase-mediated pathway, J. Cell. Mol. Med. 14 (2010) 2025.

[43] R. Willumeit, M. Kumpugdee, S.S. Funari, K. Lohner, B.P. Navas, K. Brandenburg, S. Linser, J. Andrä, Structural rearrangement of model membranes by the peptide antibiotic NK-2, Biochim. Biophys. Acta 1669 (2005) 125.

[44] G. Pabst, S.L. Grage, S. Danner-Pongratz, W. Jing, A.S. Ulrich, A. Watts, K. Lohner, A. Hickel, Membrane thickening by the antimicrobial peptide PGLa, Biophys. J. 95 (2008) 5779.

[45] A.H.S. Martinelli, K. Kappaun, R. Ligabue-Braun, M.S. Defferrari, A.R. Piovesan, F. Stanisçuaski, D.R. Demartini, C.A. Dal Belo, C.G.M. Almeida, C. Follmer, H. Verli, C.R. Carlini, G. Pasquali, Structure–function studies on jaburetox, a recombinant insecticidal peptide derived from jack bean (*Canavalia ensiformis*) urease, Biochim. Biophys. Acta 1840 (2014) 935.

[46] E. Staudegger, E.J. Prenner, M. Kriechbaum, G. Degovics, R.N.A.H. Lewis, R.N. McElhaney, K. Lohner, X-ray studies on the interaction of the antimicrobial peptide gramicidin S with microbial lipid extracts: evidence for cubic phase formation, Biochim. Biophys. Acta 1468 (2000) 213.

[47] E. Sevcsik, G. Pabst, A. Jilek, K. Lohner, How lipids influence the mode of action of membrane-active peptides, Biochim. Biophys. Acta 1768 (2007) 2586.

[48] C. Guo, S. Liu, Z. Dai, C. Jiang, W. Li, Polydiacetylene vesicles as a novel drug sustained-release system, Colloids Surf. B Biointerfaces 76 (2010) 362.

[49] O. Wesołowska, K. Michalak, J. Maniewska, A.B. Hendrich, Giant unilamellar vesicles – a perfect tool to visualize phase separation and lipid rafts in model systems, Acta Biochim. Pol. 56 (2009) 33.

[50] R. Dimova, S. Aranda, N. Bezlyepkina, V. Nikolov, K.A. Riske, R. Lipowsky, A practical guide to giant vesicles. Probing the membrane nanoregime via optical microscopy, J. Phys. Condens. Matter 18 (2006) S1151.

[51] C. Barja-Fidalgo, J.A. Guimarães, C.R. Carlini, Lipoxygenase-mediated secretory effect of canatoxin the toxic protein from *Canavalia ensiformis* seeds, Toxicon 29 (1991) 453.

[52] M.S. Defferrari, R. da Silva, I. Orchard, C.R. Carlini, Jack bean (*Canavalia ensiformis*) urease induces eicosanoid-modulated hemocyte aggregation in the Chagas' disease vector *Rhodnius prolixus*, Toxicon 82 (2014) 18.

[53] C.R. Carlini, C. Gomes, J.A. Guimaraes, R.P. Markus, H. Sato, G. Trolin, Central nervous effects of the convulsant protein canatoxin, Acta Pharmacol. Toxicol. 54 (1984) 161.

[54] S.A. Sanchez, L.A. Bagatolli, E. Gratton, T.L. Hazlett, A two-photon view of an enzyme at work: crotalus atrox venom PLA2 interaction with single-lipid and mixed-lipid giant unilamellar vesicles, Biophys. J. 82 (2002) 2232.

[55] E.F. Pettersen, T.D. Goddard, C.C. Huang, G.S. Couch, D.M. Greenblatt, E.C. Meng, T.E. Ferrin, UCSF Chimera – a visualization system for exploratory research and analysis, J. Comput. Chem. 25 (2004) 1605.

[56] N.A. Baker, D. Sept, S. Joseph, M.J. Holst, J.A. McCammon, Electrostatics of nanosystems: application to microtubules and the ribosome, Proc. Natl. Acad. Sci. U. S. A. 98 (2001) 10037.

[57] J. Kyte, R.F. Doolittle, A simple method for displaying the hydropathic character of a protein, J. Mol. Biol. 157 (1982) 105.

[58] Predictor Of Naturally Disordered Regions, Pondr software, www.pondr.com (2015).